



# Efficient targeted mutation of genomic essential genes in yeast *Saccharomyces cerevisiae*

Shan Yang<sup>1,2,3</sup> · Xuan Cao<sup>1</sup> · Wei Yu<sup>1</sup> · Shengying Li<sup>4</sup> · Yongjin J. Zhou<sup>1,2,5</sup> 

Received: 9 November 2019 / Revised: 13 January 2020 / Accepted: 23 January 2020 / Published online: 11 February 2020  
© Springer-Verlag GmbH Germany, part of Springer Nature 2020

## Abstract

Targeted gene mutation by allelic replacement is important for functional genomic analysis and metabolic engineering. However, it is challenging in mutating the essential genes with the traditional method by using a selection marker, since the first step of essential gene knockout will result in a lethal phenotype. Here, we developed a two-end selection marker (Two-ESM) method for site-directed mutation of essential genes in *Saccharomyces cerevisiae* with the aid of the CRISPR/Cas9 system. With this method, single and double mutations of the essential gene *ERG20* (encoding farnesyl diphosphate synthase) in *S. cerevisiae* were successfully constructed with high efficiencies of 100%. In addition, the Two-ESM method significantly improved the mutation efficiency and simplified the genetic manipulation procedure compared with traditional methods. The genome integration and mutation efficiencies were further improved by dynamic regulation of mutant gene expression and optimization of the integration modules. This Two-ESM method will facilitate the construction of genomic mutations of essential genes for functional genomic analysis and metabolic flux regulation in yeasts.

## Key Points

- A Two-ESM strategy achieves mutations of essential genes with high efficiency of 100%.
- The optimized three-module method improves the integration efficiency by more than three times.
- This method will facilitate the functional genomic analysis and metabolic flux regulation.

**Keywords** Site-directed mutation · Essential gene · Genome editing · CRISPR/Cas9 · Yeast

Dedicated to the 70th anniversary of Dalian Institute of Chemical Physics, Chinese Academy of Sciences

**Electronic supplementary material** The online version of this article (<https://doi.org/10.1007/s00253-020-10405-5>) contains supplementary material, which is available to authorized users.

✉ Yongjin J. Zhou  
zhouyongjin@dicp.ac.cn

<sup>1</sup> Division of Biotechnology, Dalian Institute of Chemical Physics, Chinese Academy of Sciences, 457 Zhongshan Road, Dalian 116023, China

<sup>2</sup> Dalian Key Laboratory of Energy Biotechnology, Dalian Institute of Chemical Physics, Chinese Academy of Sciences, Dalian 116023, China

<sup>3</sup> University of Chinese Academy of Sciences, Beijing 100049, China

<sup>4</sup> Shandong Provincial Key Laboratory of Synthetic Biology, CAS Key Laboratory of Biofuels, Qingdao Institute of Bioenergy and Bioprocess Technology, Chinese Academy of Sciences, No. 189 Songling Road, Qingdao 266101, Shandong, China

<sup>5</sup> CAS Key Laboratory of Separation Science for Analytical Chemistry, Dalian Institute of Chemical Physics, Chinese Academy of Sciences, Dalian 116023, China

## Introduction

The development of microbial cell factories is considered one of the feasible approaches for sustainable supply of chemicals, biofuels and pharmaceuticals (Ebert et al. 2018; Eichenberger et al. 2018; Meadows et al. 2016; Nielsen and Keasling 2016). For this purpose, it is essential to efficiently redirect carbon fluxes toward products of interest by comprehensive metabolic engineering (Hong et al. 2019), which involves reconstructing heterologous biosynthetic pathways (Brown et al. 2015; Trantas et al. 2009), overexpressing the rate-limiting steps (Dai et al. 2013; Donald et al. 1997; Zhou et al. 2012), elimination of the feedback inhibition (Engels et al. 2008; Luttkik et al. 2008; Zhou et al. 2016) and/or downregulating competing pathways (Brown et al. 2015; Rodriguez et al. 2015). Recently, several advanced genetic editing tools have been developed for rapidly constructing and optimizing biosynthetic pathways in microbial cell factories (Lv et al. 2019; Wijsman et al. 2019; Wong et al. 2017).

In general, downregulating competing pathways are implemented by knocking out the pathway relating genes, which however may lead to lethal or auxotrophic phenotypes (Anderson et al. 1989; Compagno et al. 1996; Jennings et al. 1991). Lethality clearly prohibits cell factory construction and auxotrophy brings high-cost supplementation of essential nutrients in industrial processes. Downregulating the gene expression through promoter replacement is an alternative approach to repress the competing pathways. For example, in *Saccharomyces cerevisiae*, downregulating the expression of *ERG9* (squalene synthase encoding gene) in the sterol biosynthetic pathway, through replacing its native promoter with a weak or conditionally repressed promoters, succeeded in improving the sesquiterpene production with enhanced supply of the precursor farnesyl diphosphate (FPP) and repressed competitive sterol biosynthesis (Asadollahi et al. 2008; Paddon et al. 2013; Scalcinati et al. 2012; Xie et al. 2015). However, some bifunctional enzymes such as ERG20p can synthesize both geranyl diphosphate (GPP, C10) and FPP (C15) by consecutive condensation of C5 units isopentenyl diphosphate (IPP) and dimethylallyl diphosphate (DMAPP) in the mevalonate (MVA) pathway (Withers and Keasling 2007). It is challenging to improve the monoterpene production by downregulation of *ERG20*, which cannot prevent GPP consumption toward FPP synthesis (Fischer et al. 2011; Oswald et al. 2007). Indeed, replacement of the native *ERG20* promoter with a weaker promoter resulted in a reduced monoterpene production (Zhao et al. 2017), which might be attributed to the reduced supply of precursor GPP (see blue part in Supplemental Fig. S1). Some exogenous GPP synthases showed a specific GPPS activity in vitro, which however failed in improving

monoterpene production in yeast (Zhao et al. 2016), due to the strong competition from the wild-type ERG20p. Engineering the ERG20p variants, toward high specific GPP synthase with low activity toward FPP synthesis, significantly increased the production of monoterpenes (Fischer et al. 2011; Ignea et al. 2014; Zhao et al. 2016). Allelic replacement of the wild-type *ERG20* with its mutants would help to construct a genetically stable strain for redirecting metabolic fluxes toward monoterpene biosynthesis (see red part in Supplemental Fig. S1). More importantly, allelic replacement of the essential gene to create a mutant is crucial for functional genomic analysis (Yang et al. 2020; Zhang et al. 2015).

*ERG20* is an essential gene for anabolic metabolism of downstream cellular components including sterols, dolichols, and ubiquinone (Anderson et al. 1989; Szkopińska et al. 1997; Szkopińska and Plochocka 2005), which are essential membrane components or an important component of the electron transfer system (Hartmann 1998; Okada et al. 1998; Sato et al. 1999). So the key role of the *ERG20* gene in cell growth makes its allelic replacement rather challenging (see green part in Supplemental Fig. S1). In general, a plasmid expressing the wild-type essential gene is usually transformed into cells to ensure normal growth before the knockout of the chromosomal wild-type essential gene (steps 1–2 in Fig. 1a). The essential gene can be deleted using a selection marker such as *URA3* (step 3 in Fig. 1a) and then the mutated gene can be introduced by replacing the selection marker under counter selection stresses (such as 5-FOA for *URA3* exclusion) or CRISPR/Cas9 system (step 4 in Fig. 1a). Finally, the plasmid carrying the essential gene or the guide RNA (gRNA) plasmid can be removed (step 5 in Fig. 1a). This traditional system is complicated and an additional copy of the wild-type gene on the plasmid may cause reverse mutation via homologous recombination.

Here, we developed a two-end selection marker (Two-ESM) method with the aid of the CRISPR/Cas9 system for rapid site-directed mutagenesis of essential genes in the *S. cerevisiae* genome by using *ERG20* as a model gene. At the first step, we directly replaced the wild-type *ERG20* with the *ERG20*<sup>N127W</sup> and *ERG20*<sup>A99W, N127W</sup> by integration of one module or three modules harboring the mutants with two flanked selection markers such as *HIS3* and *amdSYM* (Solis-Escalante et al. 2013) (steps 1 and 2 in Fig. 1b, Fig. 4a). Then the two flanked selection markers were simultaneously removed with the CRISPR/Cas9 system (step 3 in Fig. 1b). This Two-ESM system was capable of introducing single and double mutations (*ERG20*<sup>N127W</sup> and *ERG20*<sup>A99W, N127W</sup>) with high efficiency of 100%. Finally, this convenient Two-ESM strategy was also applied to target mutagenesis of *CDC19* gene (encoding pyruvate kinase 1 PYK1p), suggesting that this method should facilitate precise pathway engineering and functional genomic analysis in *S. cerevisiae* and even other yeasts.

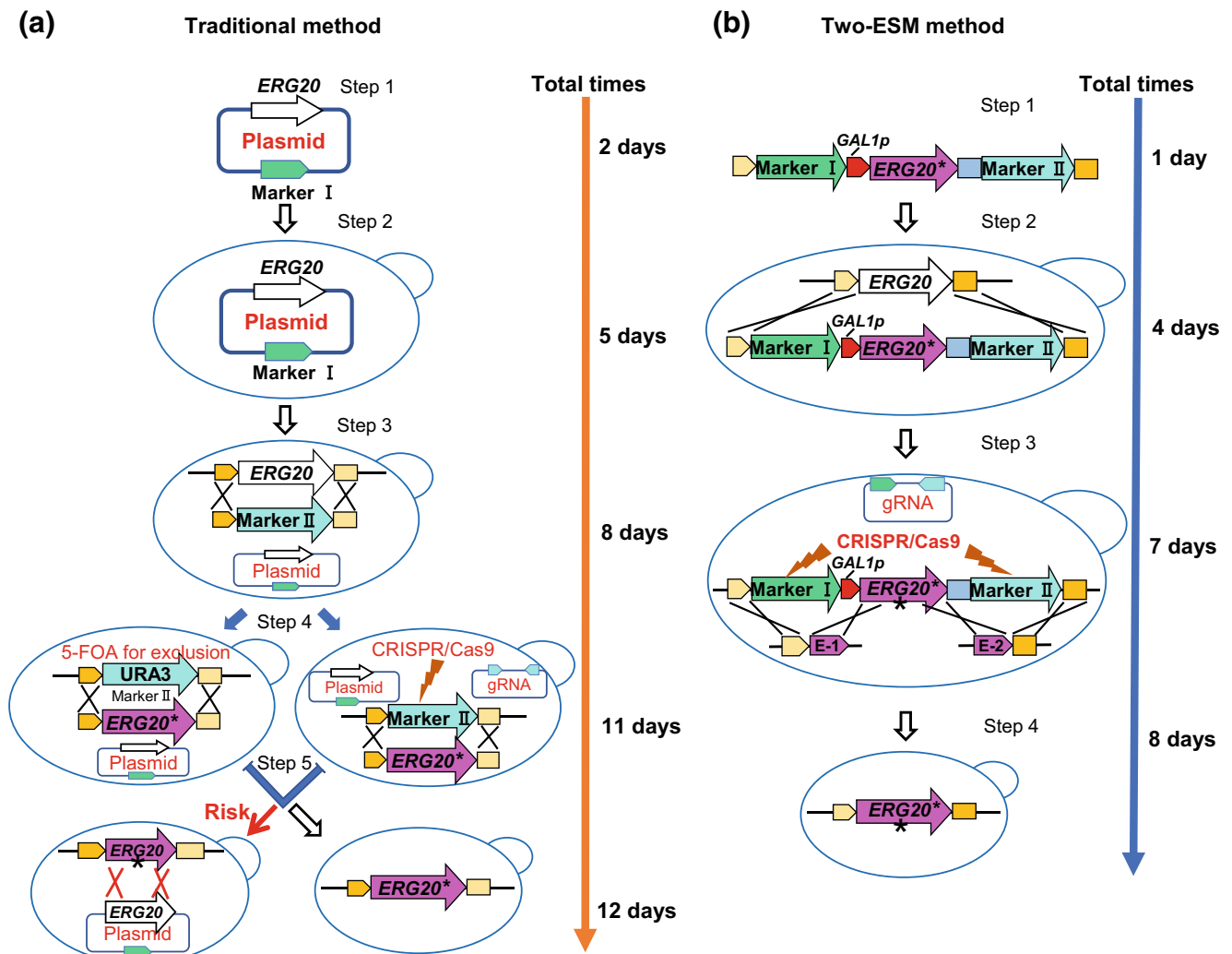


**Fig. 1** Schematic diagram of steps for mutating an essential gene on the chromosome by using *ERG20* as an example. **a** The traditional method: Step 1 is to construct a plasmid harboring wild-type *ERG20*, which is then transformed into yeast cells (step 2). Step 3 is to replace the genomic wild-type *ERG20* by using a selection marker such as *URA3*. Then the mutant *ERG20\** is genomically integrated to replace the selection marker *URA3* by using 5-FOA for *URA3* exclusion or using the CRISPR/Cas9 system (step 4). The blue arrow indicates that there are two different ways to remove the selection marker in this step. Step 5 is to lose the plasmid containing wild-type *ERG20* or the gRNA plasmid. There is a risk of homologous recombination between the mutant genome-integrated

*ERG20\** and the wild-type *ERG20* carried in the plasmid, which may lead to changing the mutant *ERG20\** back to the wild-type *ERG20* (the red arrow). The red line indicates possible homologous recombination in this step. **b** Mutating *ERG20* gene by the Two-ESM method: Step 1 is to construct the module containing the mutant *ERG20\**. Step 2 is to integrate the module to the chromosome by homologous recombination. Step 3 is to remove the two selection markers with the efficient CRISPR/Cas9 system. E-1 and E-2 represent the part sequence of the *ERG20\** gene. Step 4 is to lose the gRNA plasmid. Each step has a corresponding number of experimental days and the total are also shown on the right side

## Materials and methods

### Strains, plasmids, and reagents

Strains and plasmids used in this study were listed in Supplemental Table S1 and Table S2, respectively. PrimeStar DNA polymerase was purchased from TaKaRa Bio (Dalian, China).  $2 \times$  Taq Master Mix (Dye Plus), ClonExpress II One Step Cloning Kit, and ClonExpress MultiS One Step Cloning Kit were purchased from Vazyme Biotech (Nanjing, China). DNA gel purification and plasmid extraction kits were supplied by OMEGA (Norcross, USA).

All oligonucleotides (Supplemental Table S3) were synthesized at Sangon Biotech (Shanghai, China). Yeast extracts, tryptone, agar powder, and peptone were from Sangon Biotech. All other chemicals were purchased from Sangon Biotech unless stated otherwise.

### Strain cultivation

Unless otherwise specified, *Escherichia coli* cells were grown at 37 °C and 220 rpm (Zhichu Shaker ZQZY-CS8) on Luria-Bertani (LB) medium (10 g/L tryptone, 5 g/L yeast extract, 10 g/L NaCl). A total of 100 mg/L of ampicillin was normally

supplemented for plasmid maintenance. Yeast strains were generally cultivated in YPD media consisting of 10 g/L yeast extract, 20 g/L peptone, and 20 g/L glucose. A total of 200 mg/L G418 was used for selection of transformants harboring a *KanMX* cassette. Strains containing *URA3* based plasmids were selected on synthetic complete media without uracil (SC-URA), which consisted of 6.7 g/L yeast nitrogen base (YNB) without amino acids and 20 g/L glucose. The *URA3* marker was recycled on SC+5FOA plates containing 6.7 g/L YNB, 20 g/L glucose, and 1 g/L 5-fluoroorotic acid (5-FOA). Strains containing a *HIS3* based cassette were cultured in SG-HIS (synthetic complete medium with 20 g/L galactose as carbon source and histidine omitted). Strains containing the *amdSYM* cassette (Solis-Escalante et al. 2013) were selected on SM media (3 g/L  $\text{KH}_2\text{PO}_4$ , 0.5 g/L  $\text{MgSO}_4 \cdot 7\text{H}_2\text{O}$ , 6.6 g/L  $\text{K}_2\text{SO}_4$ , 0.6 g/L acetamide, 20 g/L glucose or galactose) with trace metal and vitamin solutions (Verduyn et al. 1992). All the above media were supplemented with 40 mg/L histidine and/or 60 mg/L uracil if needed. 20 g/L agar was added to make solid media. Yeast cells were cultivated at 30 °C and 220 rpm in liquid media.

### Strain construction

Transformation of *E. coli* was performed according to a previously described protocol (Inoue et al. 1990). All *S. cerevisiae* strains used in this study were derived from CEN.PK113-11C (*MATa SUC2 MAL2-8c his3Δ1 ura3-52*). For constructing a CRISPR/Cas9 system, the module containing the *Cas9* gene and the *KanMX* expression cassette was amplified from the pECAS9-gRNA-KanMX-tHFD1 plasmid (Zhu et al. 2017) and integrated into the genomic XI-5 site (Mikkelsen et al. 2012) by homologous recombination (the resulting strain SY01). Then, the *KanMX* targeting gRNA expression plasmid and the repair fragment were transformed into SY01 for removing of *KanMX* marker. Amplification primers and repair primers are shown in Supplemental Table S3.

Site-directed mutagenesis of *ERG20* or *CDC19* was performed by PCR using oligonucleotides introducing the respective mutation (Ho et al. 1989). The integration modules were assembled by one-pot fusion PCR as previously described (Zhou et al. 2012). In spite of single or double mutations, the module containing one selection marker was called the one-end selection marker method (One-ESM), while the module with two selection markers was called the two-end selection marker (Two-ESM). *HIS3* and *amdSYM* selection markers were mainly used in this study. The DNA cassettes or plasmids were transformed to *S. cerevisiae* by using the chemical transformation protocol (Duan et al. 2019).

### Plasmid construction

Initially, a new gRNA plasmid was constructed using the pROS10 plasmid (Mans et al. 2015) as a template with two primers (P6 and P7 in Supplemental Fig. S2a) containing the 20-bp recognition sequences to obtain the module including the gRNA expression cassette and the 2- $\mu\text{m}$  sequence, and a single primer (6005 in Supplemental Fig. S2a) binding at each of the two SNR52 promoters to obtain a linearized plasmid backbone. The two fragments were combined using a One Step Cloning Kit, followed by transformation to *E. coli* for screening by ampicillin resistance encoded on the plasmid backbone. Determining the specific 20 bp sequence was the most critical, which could be referred to by some gRNA scoring websites (<http://yeastriction.tnw.tudelft.nl>). In this paper, the backbone sequence arrangement and the plasmid assembly method were optimized based on the pROS10 sequences. First, ampicillin expression cassette was integrated into the fragment to replace the 2- $\mu\text{m}$  sequence (Supplemental Fig. S2B). Then, we performed the construction of pYSg4 on the basis of pYSg3, using two complementary primers P10 and P11 with a length of 59 bp, which were located in the middle of the *bla* (ampicillin resistance) gene, to split the expression module containing the 20 bp specific sequence into two parts (Supplemental Fig. S2c). These two fragments were named part 1 and part 2, and the length of primers P8/P9 containing specific 20-bp sequences was shortened to P4/P6, from 120 to 69 bp. Part 1 was amplified using the primers P8/P10, part 2 was amplified by the primers P9/P11, and backbone still was amplified with the 6005 primer. These three fragments were assembled into plasmids by the MultiS One Step Cloning Kit in vitro, and the assembled mix were transformed into *E. coli*. All plasmids were verified by DNA sequencing.

### Verification of the mutant strain

Selected yeast colonies (eight to ten) from the agar plates were cultured in 2 mL of corresponding liquid medium at 30 °C for 24 to 48 h. Then, 100  $\mu\text{l}$  of culture broth were taken for genomic DNA extraction by a quick extraction method (Looke et al. 2011). The module integration of the chromosome in the mutant strain was verified by colony PCR. Based on the correct colony PCR verification, the ORF (open reading frame) sequence of a mutant gene was amplified for sequencing, and the sequencing results directly showed whether the strain was mutated successfully. The mutation efficiency in this study is the ratio of the number of mutant strains containing mutated genes to the number of total sequenced strains.

## Results

### Strong promoter driving *ERG20* mutants for improving cellular fitness

The *ERG20*<sup>N127W</sup> has a severely reduced enzyme activity for FPP synthesis (Ignea et al. 2014) and thus retards the yeast cell growth, which would make it challenging in allelic replacement of wild-type *ERG20* with this mutant. Indeed, direct induced expression of the *ERG20*<sup>N127W</sup> cassette by the native *ERG20* promoter resulted in the absence of colonies on the plate (Fig. 2a), which suggested that a high level of FPPS activity was essential for homologous recombination. We thus leveraged a strong galactose induced promoter *GAL1p* to enhance the expression of the *ERG20*<sup>N127W</sup> and achieved the normal growth of cells with 20 g/L galactose during gene replacement (step 1 and 2, Fig. 1b). The *GAL1p* driving *ERG20*<sup>N127W</sup> cassette rescued the cell growth in the plates with dozens of colonies (Fig. 2b). Then the *GAL1p* was removed together with the selection markers by using the CRISPR/Cas9 system and the native *ERG20* promoter was left for expressing *ERG20*<sup>N127W</sup> (step 3 in Fig. 1b). This result clearly showed that a temporary strong induced promoter significantly improved the integration efficiency of gene cassettes carrying gene mutants with low enzyme activities and that it achieved site-directed mutagenesis of essential genes.

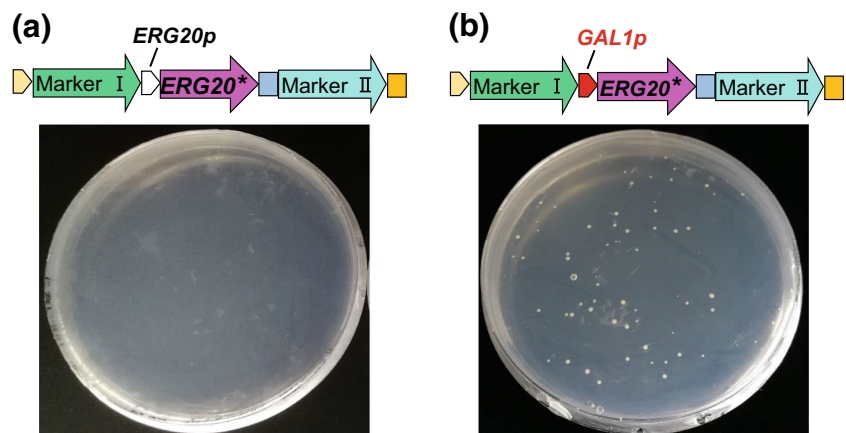
### One-end and two-end selection marker method

A selection marker is essential for targeted integration of DNA fragments and a one-end selection marker (One-ESM) is usually enough for genome integration of normal fragments. However, One-ESM may have negative partial DNA fragment recombination during allelic replacement of site-directed mutants, especially if the site-directed mutants adversely affect cellular fitness (Fig. 3a). Actually, though the colony PCR analysis showed that there were identical 100% positive integration efficiency

(Supplemental Fig. S3), DNA sequencing (Supplemental Fig. S4) showed that the One-ESM methods, with *amdSYM* as a back-end selection marker (strains SY04) and *HIS3* as a front-end selection marker (strains SY05), had only a 0% and 30% positive mutation efficiency, respectively (Fig. 3c). These data suggested that partial DNA fragment recombination took place when using One-ESM. In detail, when the selection marker is located at the front end, the front part of *ERG20*<sup>N127W</sup> mutation site might undergo a homologous recombination with the genome (see right part with red lines in Fig. 3a), resulting in the failed integration into the mutation site. Similarly, when the marker is on the back end, the posterior ORF sequence of the *ERG20*<sup>N127W</sup> site may also be homologously recombined with the genome (see left part with red lines in Fig. 3a). In particular, the integration of *ERG20*<sup>N127W</sup> conferred stresses for the cell growth due to its severely weak activity for FPP synthesis, which would make it challenging for integration of the correct mutation compared to non-sense homologous recombination with no growth stress. It is worth mentioning that the front-end method used the *GAL1* promoter to express *ERG20*<sup>N127W</sup>, while the back-end method used a weak *ERG20* promoter (Fig. 3a). The higher mutation efficiency of *GAL1* promoter containing *ERG20*<sup>N127W</sup> further confirmed that using a strong promoter for temporary inducing the expression of *ERG20*<sup>N127W</sup> could not only enhance the integration efficiency but also increase the mutation rate.

Thus, we developed a two-end selection marker (Two-ESM) mediated recombination strategy that could clamp the site-directed mutants to replace the wild-type gene by using two selection stresses (Fig. 3b). This Two-ESM method, with *HIS3* and *amdSYM* as flanked markers, enabled a 100% mutation efficiency, which suggested that the Two-ESM method succeeds in clamping the *ERG20*<sup>N127W</sup> to replace the wild-type *ERG20*, even though *ERG20*<sup>N127W</sup> confers strong stress on cell growth. However, the two-ESM

**Fig. 2** Temporary induced expression of *ERG20*<sup>N127W</sup> by *GAL1p* enabled genome integration of *ERG20*<sup>N127W</sup>. The impact of the *ERG20*<sup>N127W</sup> expression induced by the native *ERG20* promoter (a) or the strong *GAL1* promoter (b) respectively on transformation results in the Two-ESM method



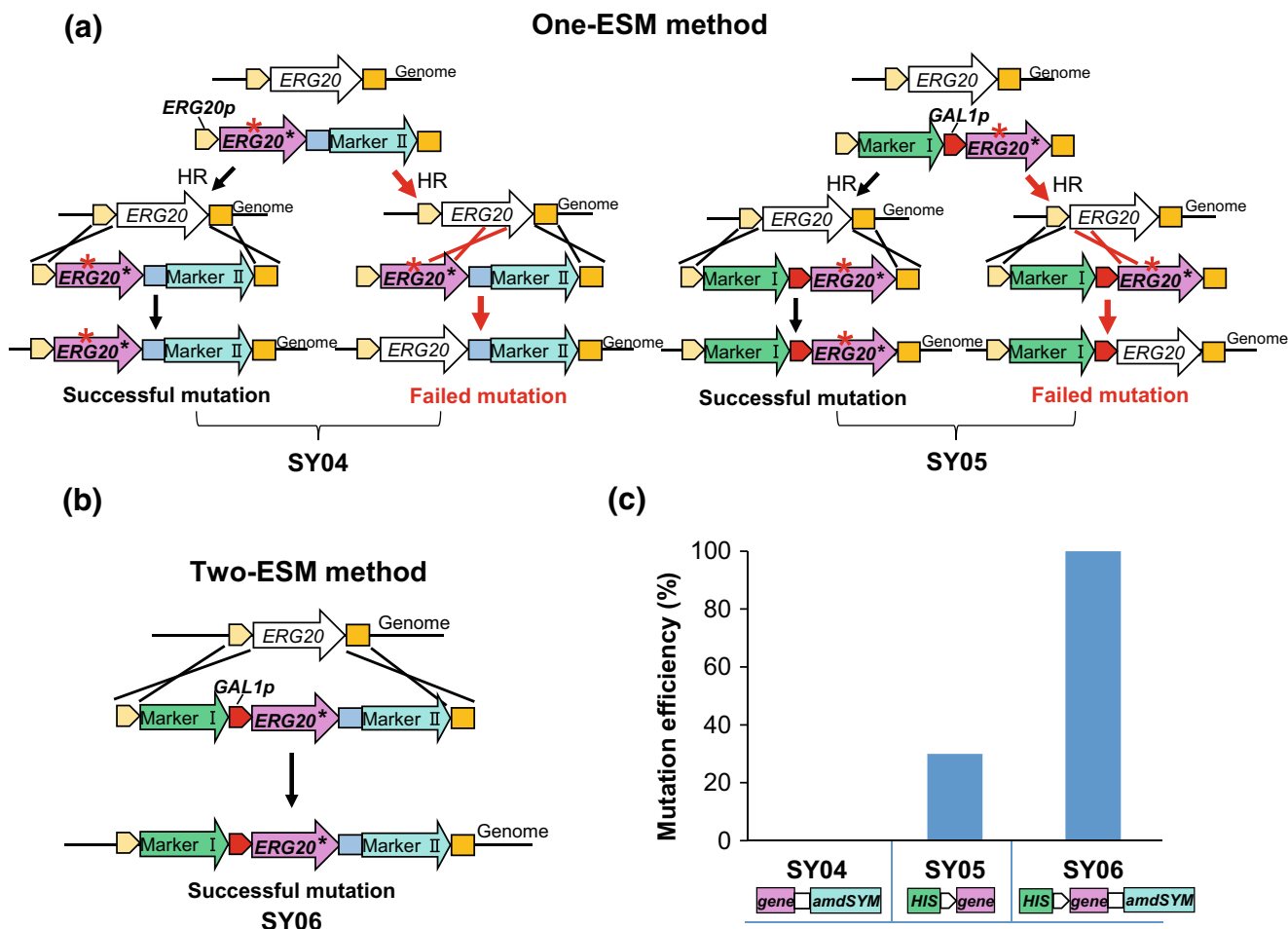


**Fig. 3** The mutation efficiencies of *ERG20\** when using One-ESM and Two-ESM methods. **a** The homologous recombination diagram of SY04 and SY05 strains obtained by the One-ESM method. The left part shows that the selection marker is located at the back end of mutant *ERG20\**, which is induced to express by the *ERG20* promoter (strains SY04). The right part shows that the selection marker is located at the front end of mutant *ERG20\**, which is induced to express by the *GAL1* promoter (strains SY05). Both SY04 and SY05 strains had two possible homologous recombination processes, and the processes of successful

and failed mutations are represented by black and red arrows, respectively. Black solid lines indicate desired homologous recombination and red lines indicate undesired homologous recombination. The red mark \* indicates the site of the mutation. **b** The homologous recombination diagram of SY06 strains obtained by the Two-ESM method. The black arrow and black solid lines indicate the homologous recombination process with successful mutations. **c** The mutation efficiencies of One-ESM and Two-ESM methods. Single mutation efficiency of *ERG20<sup>N127W</sup>* in SY04, SY05 and SY06 strains

method produced fewer colonies as compared with the One-ESM method (Supplemental Fig. S5), which might be attributed to the difficulties in the integration of a larger module of a two-ESM integrating cassette.

**Multi-module assembly increased integration efficiency**

Although the mutation efficiency of the Two-ESM method was higher than that of the One-ESM method, the number of transformants was obviously reduced (Supplemental Fig. S5). It was likely that the large module in the Two-ESM method led to the reduction of integration efficiency. We thus divided our large fusion fragment (Fig. 4a) into three modules, which was

called three-module strategy, which enabled a 3-fold higher integration efficiency in the single mutation of *ERG20<sup>N127W</sup>* in comparison with that of one-module strategy (Fig. 4b). While introducing the double mutation of *ERG20<sup>A99W, N127W</sup>*, the three-module strategy showed a 3.7-fold improvement of integration efficiency compared with one-module strategy (Fig. 4c). Furthermore, we observed a slight improvement in mutation efficiency using three-module strategy (100%) compared with one-module strategy (93%, Fig. 4c and Supplemental Fig. S6). This result clearly showed that the three-module strategy improved the integration and mutation efficiencies and the Two-ESM method was applicable in double mutation of the lethal gene with a high efficiency of 100%.

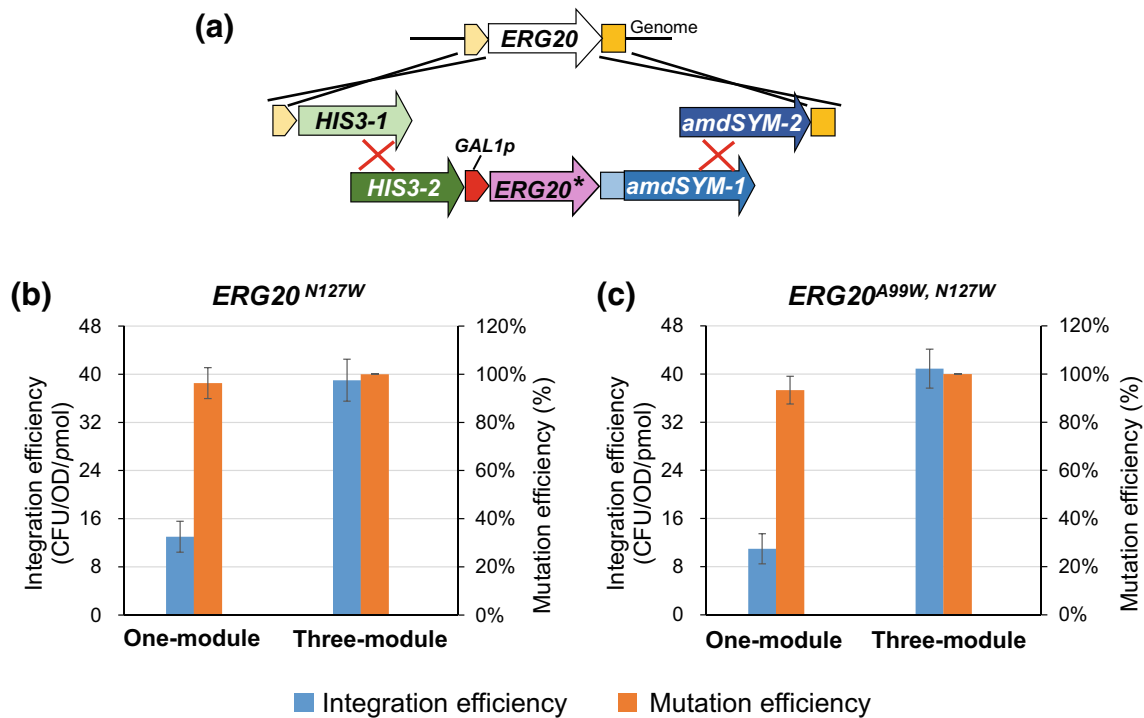


**Fig. 4** Three-module strategy improved the genomic integration of *ERG20* mutant (*ERG20\**) cassette. **a** Schematic diagram of three-module strategy. The one-module is divided into three parts by splitting two selection markers into two segments. Then two broken selection markers are in vivo assembled into the complete gene by homologous

recombination. **b** The integration and mutation efficiencies of *ERG20*<sup>N127W</sup> by using one-module and three-module strategies. **c** The integration and mutation efficiencies of *ERG20*<sup>A99W, N127W</sup>. All data represent the mean ± s.d. of biological triplicates

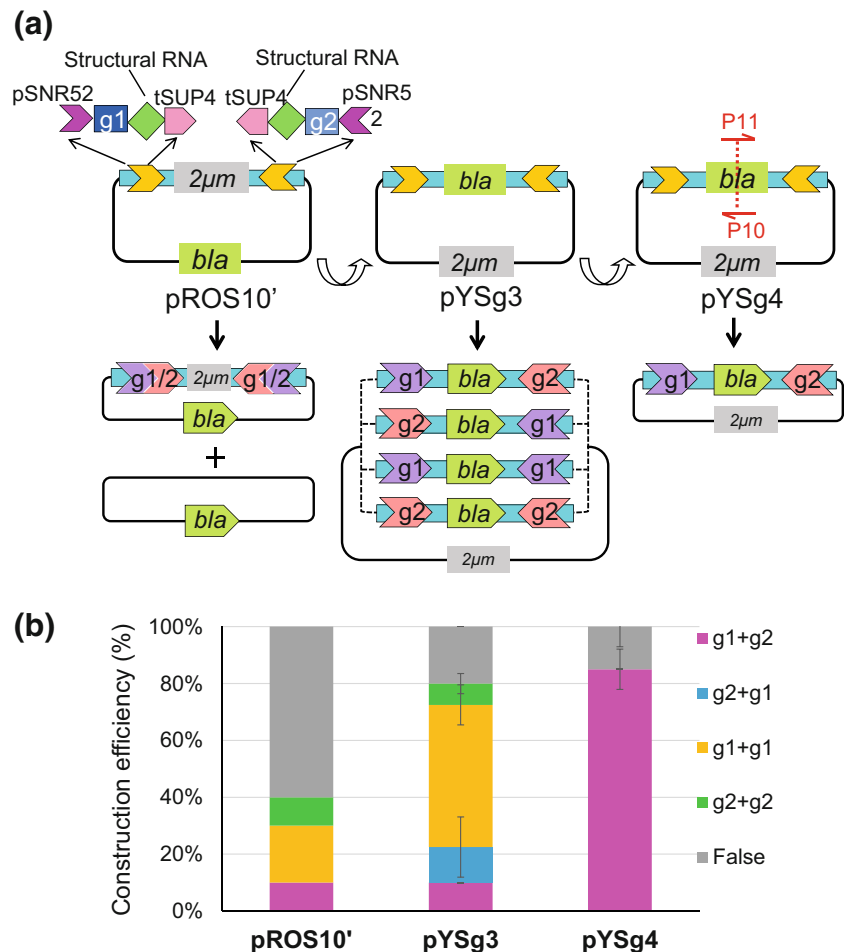
### Simultaneous removing two selection markers with the efficient CRISPR/Cas9 system

Simultaneous removing the two markers flanked the gene mutants is required for seamless site-directed mutagenesis of the target gene. Counter selection markers such as *URA3* have been successfully used for seamless genome manipulation (Akada et al. 2006; Zhou et al. 2011), however, it is challenging to simultaneously remove two selection markers as there is low frequency in natural chromosome breaking. Thanks to the CRISPR/Cas9 system that can break the target double-strand DNA sequence with high frequency and specificity (Mans et al. 2018), we may seamlessly remove the two marker genes with the aid of homologous recombination with an enhanced-specificity Cas9 nuclease variant from *Streptococcus pyogenes* (Slaymaker et al. 2016).

We first optimized a plasmid for simultaneous expression of two guide RNAs (gRNAs), which is essential for precise genome editing. The pROS10 plasmid has been constructed for simultaneous expression of two gRNAs (Mans et al. 2015), which contains two gRNA expression modules that are back-to-back flanked at the 2- $\mu$ m replication sequence. This kind of element arrangement had a high level of false assembled constructs, since the plasmid backbone could cyclize without assembling the gRNA expression module and the 2- $\mu$ m sequence, and there was no selection marker kicking

out these false constructs during plasmid assembly in *E. coli* (pROS10', plasmids Fig. 5a). We thus swapped the location of the *bla* (for ampicillin resistance) and the 2- $\mu$ m replication sequence, which enabled the picking out the successfully assembled gRNA plasmid under the ampicillin stress. Indeed, new plasmids pYSg3 led to a 2-fold higher positive ratio in harboring gRNAs than that of pROS10' (Fig. 5b). We then tried to improve the targeted double gRNAs assembly in the plasmid. In the previous protocol, the gRNAs were integrated through PCR amplification of the selection marker *bla* with end-end structural gRNA by using primers P4 and P6 (Supplemental Fig. S2b) and the PCR fragment was assembled into plasmids pYSg3. However, the primers P4 and P6 had an identical sequence in the structural gRNA part, binding to Cas9, which resulted in random combinations of two 20-bp recognition sequences of P4 and P6 and hence four different possible plasmids with a low assembly specificity (plasmids pYSg3 in Fig. 5a). Indeed, this gRNA plasmid assembly method obtained four types of plasmids (g1+g2, g2+g1, g1+g1, g2+g2), and two gRNA integration plasmids (g1+g2 and g2+g1) had only a small ratio of 22.5%, which made it challenging to pick out the targeted plasmids. To improve the specificity of simultaneous integration of two gRNAs g1 and g2, we split the *bla* fragment and amplified the two fragments separately by using the *bla* inner binding primers P10 and P11 (P8/P10 for part 1 and P9/P11 for part 2, Supplemental Fig.

**Fig. 5** Optimizing gRNA expressing plasmids for simultaneously expressing two gRNAs. **a** pROS10 is the initial plasmid used as a template to amplify the gRNA expression cassette and backbone. It may assemble empty plasmid without gRNAs in resulting plasmid mix pROS10', since there is no selection stress during in vivo plasmid assembly in *E. coli*. To ensure gRNA assembly, *bla* marker was placed in the middle of the gRNA expression cassette (plasmids pYSg3), which mainly assemble four possible gRNA combinations (g1/g2, g2/g1, g1/g1, g2/g2). Further splitting at the middle of *bla* for in vivo assembly can ensure specific gRNA assembly (for example g1/g2 in plasmids pYSg4). **b** The gRNA combinations in three plasmid assembly: g1/g2, g2/g1, g1/g1, g2/g2, and false. The data represent the mean  $\pm$  s.d. of biological triplicates



S2c). Then these two DNA fragments were assembled into the backbone from the pYSg3 plasmid and only the correctly assembled *bla* with g1 and g2 rendered the ampicillin resistance during colony selection. This modified method enabled simultaneously specific assembly of two gRNAs (g1+g2) with a positive rate of 85.0%, a 3.8-fold improvement compared with the traditional plasmid assembly without a split of *bla* (Fig. 5b). Furthermore, the length of the primers P8/P9 in the method of constructing the plasmid pYSg4 was nearly 33% shorter than that of P4/P6 in the previous method, saving the costs in long primer synthesis. This specific gRNA assembly method should facilitate the integration of multiple gRNAs for multiplex genome editing. Finally, this gRNA plasmid enabled the simultaneous removal of the two selection marker with an efficiency of 100%, and thus succeeded in the seamless gene replacement of *ERG20*.

### Application of the Two-ESM method to mutate other essential genes

We further applied this Two-ESM method to introduce mutations on other essential genes such as *PYK1* (encoding

pyruvate kinase 1, also known as *CDC19*), whose mutation has been shown to regulate glycolysis (Fenton and Blair 2002; Yu et al. 2018). We here tried to introduce a single mutation R91I or R369A, by targeted replacement of the wild-type *CDC19* with *CDC19*<sup>R91I</sup> or *CDC19*<sup>R369A</sup>. Similarly, the fusion module containing *CDC19*<sup>R91I</sup> or *CDC19*<sup>R369A</sup> was also integrated into the genome by the one-module strategy and the three-module strategy, respectively (Fig. 6a). The results showed that the three-module strategy had 3.7-fold and 3.8-fold higher efficiencies for R91I and R369A, respectively, than those of the one-module strategy (Fig. 6b, c). Similarly, the three-module strategy improved the mutation efficiency for both *CDC19*<sup>R91I</sup> and *CDC19*<sup>R369A</sup> (Fig. 6b, c and Supplemental Fig. S7). This observation demonstrated that the Two-ESM method can be widely used to mutate essential genes with high efficiency.

### Discussions

Here, we developed a two-end selection marker (Two-ESM) method for rapid and efficient site-directed mutation of

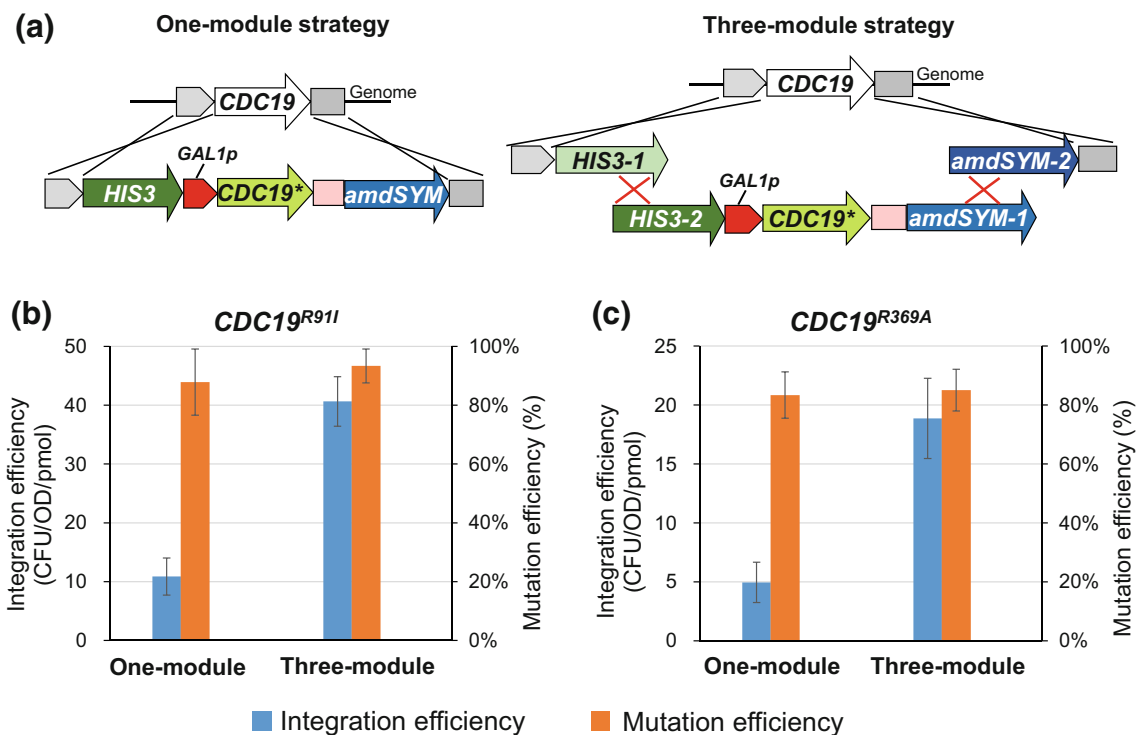


**Fig. 6** Two-ESM method mediated mutation of *CDC19\** by one-module or three-module strategies. **a** Schematic diagram one-module and three-module strategies. **b** The integration and mutation efficiencies of

genomic essential genes. Using *ERG20* as a model gene, we firstly designed the integration cassettes containing the mutation genes, two-end selection markers and homologous arms (Fig. 1b), which was used for allelic replacement of the wild-type gene. This Two-ESM method ensured the targeted mutation by homologous recombination on the flanking homologous arms, not by partially homologous recombined between the wild-type and mutation genes (Fig. 3). To compensate for the low activity of the gene mutation such as *ERG20<sup>N127W</sup>* that may retard the cell growth, we then used a strong inducible promoter *GAL1p* for temporary induced expression of the mutant in the integration cassettes and the promoter can be removed with the selection marker at the second round CRISPR/Cas9 based genome editing. We also found that dividing the integration cassette into three modules (splitting at the inner side of the selection marker) significantly improved (> 3-fold) the allelic replacement efficiency (Figs. 4 and 6). To facilitate the removal of selection markers, we optimized the gRNA assembly method (Fig. 5a), which enabled simultaneous and precise assembly of two gRNA at 85%, an 8.5-fold improvement compared with that of the previous method (Fig. 5b). With this optimized gRNA expression plasmid and CRISPR/Cas9 system, the two selection markers were simultaneously removed at a positive rate of 100%.

The traditional method not only requires the construction of a plasmid carrying the wild-type *ERG20* gene (pERG20), but also the transformation of this plasmid into *S. cerevisiae*

(Fig. 1a). Furthermore, the targeted gene mutation always involves a two-step gene replacement with the aid of a selection marker. Finally, the plasmid pERG20 needs to be lost after the replacement step. In contrast, this Two-ESM method only needs a one-step replacement (Fig. 1b). We can estimate that the total five-steps of the traditional method may cost 12 days and the Two-ESM method only needs 8 days. Though convenient single base genome editing has been developed, it however relies on limited specific nucleotide substitution between A/T and C/G (Gaudelli et al. 2017; Komor et al. 2016; Nishida et al. 2016). Moreover, CasPER was developed for mutagenesis of some essential genes in *S. cerevisiae* by combining with error-prone PCR and CRISPR/Cas9 (Jakociunas et al. 2018), which however was a random mutagenesis strategy and relies on a high-throughput screening strategy. Comparatively, this Two-ESM method can mediate target mutations at any sites of essential genes with high efficiency.

In summary, a Two-ESM method was developed for site-directed mutation of genomic essential genes, which should be useful for functional genomic analysis and metabolic engineering.

**Acknowledgments** We thank Prof. Jens Nielsen (Chalmers University of Technology) for kindly sharing the plasmid pECAS9-gRNA-KanMX-tHFD1 carrying the *Cas9* encoding gene and Prof. Jack Pronk (Delft University of Technology) for sharing the pROS10 and the *amdSYM* encoding gene.

**Author contributions** SY conducted the experiments and wrote the manuscript. XC assisted the construction of the CRISPR-Cas9 system. WY and SL assisted the designing part of experiments and revised the manuscript. YJZ conceived the study, designed the experiments and revised the manuscript.

**Funding information** This study was funded by the National Key Research and Development Program of China (2018YFA0900300), National Natural Science Foundation of China (21877111), LiaoNing Revitalization Talents Program (XLYC1807191), and the DICP&QIBEBT program (DICP & QIBEBT UN201706).

## Compliance with ethical standards

**Conflict of interest** The authors declare that they have no conflict of interest.

**Ethical approval** This article does not contain studies with human participants or animals performed by any of the authors.

## References

- Akada R, Kitagawa T, Kaneko S, Toyonaga D, Ito S, Kakihara Y, Hoshida H, Morimura S, Kondo A, Kida K (2006) PCR-mediated seamless gene deletion and marker recycling in *Saccharomyces cerevisiae*. *Yeast* 23(5):399–405
- Anderson MS, Yarger JG, Burck CL, Poulter CD (1989) Farnesyl diphosphate synthetase. Molecular cloning, sequence, and expression of an essential gene from *Saccharomyces cerevisiae*. *J Biol Chem* 264(32):19176–19184
- Asadollahi MA, Maury J, Møller K, Nielsen KF, Schalk M, Clark A, Nielsen J (2008) Production of plant sesquiterpenes in *Saccharomyces cerevisiae*: effect of *ERG9* repression on sesquiterpene biosynthesis. *Biotechnol Bioeng* 99(3):666–677
- Brown S, Clastre M, Courdavault V, O'Connor SE (2015) De novo production of the plant-derived alkaloid strictosidine in yeast. *Proc Natl Acad Sci U S A* 112(11):3205–3210
- Compagno C, Boschi F, Ranzi BM (1996) Glycerol production in a triose phosphate isomerase deficient mutant of *Saccharomyces cerevisiae*. *Biotechnol Prog* 12(5):591–595
- Dai Z, Liu Y, Zhang X, Shi M, Wang B, Wang D, Huang L, Zhang X (2013) Metabolic engineering of *Saccharomyces cerevisiae* for production of ginsenosides. *Metab Eng* 20:146–156
- Donald K, Hampton RY, Fritz IB (1997) Effects of overproduction of the catalytic domain of 3-hydroxy-3-methylglutaryl coenzyme A reductase on squalene synthesis in *Saccharomyces cerevisiae*. *Appl Environ Microbiol* 63(9):3341–3344
- Duan X, Ma X, Li S, Zhou Y (2019) Free fatty acids promote transformation efficiency of yeast. *FEMS Yeast Res* 19(7):foz069
- Ebert BE, Czarnotta E, Blank LM (2018) Physiologic and metabolic characterization of *Saccharomyces cerevisiae* reveals limitations in the synthesis of the triterpene squalene. *FEMS Yeast Res* 18(8):foy077
- Eichenberger M, Hansson A, Fischer D, Durr L, Naesby M (2018) De novo biosynthesis of anthocyanins in *Saccharomyces cerevisiae*. *FEMS Yeast Res* 18(4):foy046
- Engels B, Dahm P, Jennewein S (2008) Metabolic engineering of taxadiene biosynthesis in yeast as a first step towards Taxol (Paclitaxel) production. *Metab Eng* 10(3–4):201–206
- Fenton AW, Blair JB (2002) Kinetic and allosteric consequences of mutations in the subunit and domain interfaces and the allosteric site of yeast pyruvate kinase. *Arch Biochem Biophys* 397(1):28–39
- Fischer MJ, Meyer S, Claudel P, Bergdoll M, Karst F (2011) Metabolic engineering of monoterpene synthesis in yeast. *Biotechnol Bioeng* 108(8):1883–1892
- Gaudelli NM, Komor AC, Rees HA, Packer MS, Badran AH, Bryson DI, Liu DR (2017) Programmable base editing of AT to GC in genomic DNA without DNA cleavage. *Nature* 551(7681):464–471
- Hartmann M (1998) Plant sterols and the membrane environment. *Trends Plant Sci* 3(5):170–175
- Ho SN, Hunt HD, Horton RM, Pullen JK, Pease LR (1989) Site-directed mutagenesis by overlap extension using the polymerase chain reaction. *Gene* 77(1):51–59
- Hong J, Park S-H, Kim S, Kim S-W, Hahn J-S (2019) Efficient production of lycopene in *Saccharomyces cerevisiae* by enzyme engineering and increasing membrane flexibility and NADPH production. *Appl Microbiol Biotechnol* 103(1):211–223
- Ignea C, Pontini M, Maffei ME, Makris AM, Kampranis SC (2014) Engineering monoterpene production in yeast using a synthetic dominant negative geranyl diphosphate synthase. *ACS Synth Biol* 3(5):298–306
- Inoue H, Nojima H, Okayama H (1990) High efficiency transformation of *Escherichia coli* with plasmids. *Gene* 96(1):23–28
- Jakociunas T, Pedersen LE, Lis AV, Jensen MK, Keasling JD (2018) CasPER, a method for directed evolution in genomic contexts using mutagenesis and CRISPR/Cas9. *Metab Eng* 48:288–296
- Jennings SM, Tsay YH, Fisch TM, Robinson GW (1991) Molecular cloning and characterization of the yeast gene for squalene synthetase. *Proc Natl Acad Sci U S A* 88(14):6038–6042
- Komor AC, Kim YB, Packer MS, Zuris JA, Liu DR (2016) Programmable editing of a target base in genomic DNA without double-stranded DNA cleavage. *Nature* 533(7603):420–424
- Looke M, Kristjuhan K, Kristjuhan A (2011) Extraction of genomic DNA from yeasts for PCR-based applications. *Biotechniques* 50(5):325–328
- Luttik MAH, Vuralhan Z, Suir E, Braus GH, Pronk JT, Daran JM (2008) Alleviation of feedback inhibition in *Saccharomyces cerevisiae* aromatic amino acid biosynthesis: quantification of metabolic impact. *Metab Eng* 10(3–4):141–153
- Lv Y, Edwards H, Zhou J, Xu P (2019) Combining 26s rDNA and the Cre-loxP system for iterative gene integration and efficient marker curation in *Yarrowia lipolytica*. *ACS Synth Biol* 8(3):568–576
- Mans R, van Rossum HM, Wijsman M, Backx A, Kuijpers NG, van den Broek M, Daran-Lapujade P, Pronk JT, van Maris AJ, Daran JM (2015) CRISPR/Cas9: a molecular Swiss army knife for simultaneous introduction of multiple genetic modifications in *Saccharomyces cerevisiae*. *FEMS Yeast Res* 15(2):foy004
- Mans R, Wijsman M, Daran-Lapujade P, Daran J-M (2018) A protocol for introduction of multiple genetic modifications in *Saccharomyces cerevisiae* using CRISPR/Cas9. *FEMS Yeast Res* 18(7):foy063
- Meadows AL, Hawkins KM, Tsegaye Y, Antipov E, Kim Y, Raetz L, Dahl RH, Tai A, Mahatdejkul-Meadows T, Xu L, Zhao L, Dasika MS, Murarka A, Lenihan J, Eng D, Leng JS, Liu CL, Wenger JW, Jiang H, Chao L, Westfall P, Lai J, Ganesan S, Jackson P, Mans R, Platt D, Reeves CD, Saija PR, Wichmann G, Holmes VF, Benjamin K, Hill PW, Gardner TS, Tsong AE (2016) Rewriting yeast central carbon metabolism for industrial isoprenoid production. *Nature* 537(7622):694–697
- Mikkelsen MD, Buron LD, Salomonsen B, Olsen CE, Hansen BG, Mortensen UH, Halkier BA (2012) Microbial production of indolylglucosinolate through engineering of a multi-gene pathway in a versatile yeast expression platform. *Metab Eng* 14(2):104–111
- Nielsen J, Keasling JD (2016) Engineering cellular metabolism. *Cell* 164(6):1185–1197
- Nishida K, Arazoe T, Yachie N, Banno S, Kakimoto M, Tabata M, Mochizuki M, Miyabe A, Araki M, Hara KYJS (2016) Targeted nucleotide editing using hybrid prokaryotic and vertebrate adaptive immune systems. *Science* 353(6305):aaf8729

- Okada K, Kainou T, Matsuda H, Kawamukai M (1998) Biological significance of the side chain length of ubiquinone in *Saccharomyces cerevisiae*. FEBS Lett 431(2):241–244
- Oswald M, Fischer M, Dirninger N, Karst F (2007) Monoterpenoid biosynthesis in *Saccharomyces cerevisiae*. FEMS Yeast Res 7(3):413–421
- Paddon CJ, Westfall PJ, Pitera DJ, Benjamin K, Fisher K, McPhee D, Leavell MD, Tai A, Main A, Eng D, Polichuk DR, Teoh KH, Reed DW, Treynor T, Lenihan J, Fleck M, Bajad S, Dang G, Dengrove D, Diola D, Dorin G, Ellens KW, Fickes S, Galazzo J, Gaucher SP, Geistlinger T, Henry R, Hepp M, Horning T, Iqbal T, Jiang H, Kizer L, Lieu B, Melis D, Moss N, Regentin R, Secrest S, Tsuruta H, Vazquez R, Westblade LF, Xu L, Yu M, Zhang Y, Zhao L, Lievens J, Covello PS, Keasling JD, Reiling KK, Renninger NS, Newman JD (2013) High-level semi-synthetic production of the potent antimalarial artemisinin. Nature 496(7446):528–532
- Rodriguez A, Kildegaard KR, Li M, Borodina I, Nielsen J (2015) Establishment of a yeast platform strain for production of *p*-coumaric acid through metabolic engineering of aromatic amino acid biosynthesis. Metab Eng 31:181–188
- Sato M, Sato K, Nishikawa SI, Hirata A, Kato JI, Nakano A (1999) The yeast *RER2* gene, identified by endoplasmic reticulum protein localization mutations, encodes cis-prenyltransferase, a key enzyme in dolichol synthesis. Mol Cell Biol 19(1):471–483
- Scalcinati G, Knuf C, Partow S, Chen Y, Maury J, Schalk M, Daviet L, Nielsen J, Siewers V (2012) Dynamic control of gene expression in *Saccharomyces cerevisiae* engineered for the production of plant sesquiterpene alpha-santalene in a fed-batch mode. Metab Eng 14(2):91–103
- Slaymaker IM, Gao L, Zetsche B, Scott DA, Yan WX, Zhang F (2016) Rationally engineered Cas9 nucleases with improved specificity. Science 351(6268):84–88
- Solis-Escalante D, Kuijpers NG, Bongaerts N, Bolat I, Bosman L, Pronk JT, Daran JM, Daran-Lapujade P (2013) *amdSYM*, a new dominant recyclable marker cassette for *Saccharomyces cerevisiae*. FEMS Yeast Res 13(1):126–139
- Szkopińska A, Plochocka D (2005) Farnesyl diphosphate synthase; regulation of product specificity. Acta Biochim Pol 52(1):45–55
- Szkopińska A, Grabińska K, Delourme D, Karst F, Rytka J, Palamarczyk G (1997) Polyprenol formation in the yeast *Saccharomyces cerevisiae*: effect of farnesyl diphosphate synthase overexpression. J Lipid Res 38(5):962–968
- Trantas E, Panopoulos N, Ververidis F (2009) Metabolic engineering of the complete pathway leading to heterologous biosynthesis of various flavonoids and stilbenoids in *Saccharomyces cerevisiae*. Metab Eng 11(6):355–366
- Verduyn C, Postma E, Scheffers WA, Van Dijken JP (1992) Effect of benzoic acid on metabolic fluxes in yeasts: a continuous-culture study on the regulation of respiration and alcoholic fermentation. Yeast 8(7):501–517
- Wijsman M, Swiat MA, Marques WL, Hettinga JK, van den Broek M, Torre Cortes P, Mans R, Pronk JT, Daran JM, Daran-Lapujade P (2019) A toolkit for rapid CRISPR-SpCas9 assisted construction of hexose-transport-deficient *Saccharomyces cerevisiae* strains. FEMS Yeast Res 19(1):foy107
- Withers ST, Keasling JD (2007) Biosynthesis and engineering of isoprenoid small molecules. Appl Microbiol Biotechnol 73(5):980–990
- Wong L, Engel J, Jin E, Holdridge B, Xu P (2017) YaliBricks, a versatile genetic toolkit for streamlined and rapid pathway engineering in *Yarrowia lipolytica*. Metab Eng Commun 5:68–77
- Xie W, Ye L, Lv X, Xu H, Yu H (2015) Sequential control of biosynthetic pathways for balanced utilization of metabolic intermediates in *Saccharomyces cerevisiae*. Metab Eng 28:8–18
- Yang Z, Edwards H, Xu P (2020) CRISPR-Cas12a/Cpf1-assisted precise, efficient and multiplexed genome-editing in *Yarrowia lipolytica*. Metab Eng Commun 10:e00112
- Yu T, Zhou YJ, Huang M, Liu Q, Pereira R, David F, Nielsen J (2018) Reprogramming yeast metabolism from alcoholic fermentation to lipogenesis. Cell 174(6):1549–1558
- Zhang Y, Liu G, Engqvist MKM, Krivoruchko A, Hallström BM, Chen Y, Siewers V, Nielsen J (2015) Adaptive mutations in sugar metabolism restore growth on glucose in a pyruvate decarboxylase negative yeast strain. Microb Cell Factories 14(1):116
- Zhao J, Bao X, Li C, Shen Y, Hou J (2016) Improving monoterpene geraniol production through geranyl diphosphate synthesis regulation in *Saccharomyces cerevisiae*. Appl Microbiol Biotechnol 100(10):4561–4571
- Zhao J, Li C, Zhang Y, Shen Y, Hou J, Bao X (2017) Dynamic control of *ERG20* expression combined with minimized endogenous downstream metabolism contributes to the improvement of geraniol production in *Saccharomyces cerevisiae*. Microb Cell Factories 16(1):17
- Zhou YJ, Yang F, Zhang S, Tan H, Zhao Z (2011) Efficient gene disruption in *Saccharomyces cerevisiae* using marker cassettes with long homologous arms prepared by the restriction-free cloning strategy. World J Microb Biot 27(12):2999–3003
- Zhou YJ, Gao W, Rong Q, Jin G, Chu H, Liu W, Yang W, Zhu Z, Li G, Zhu G, Huang L, Zhao ZK (2012) Modular pathway engineering of diterpenoid synthases and the mevalonic acid pathway for miltiradiene production. J Am Chem Soc 134(6):3234–3241
- Zhou YJ, Buijs NA, Zhu Z, Qin J, Siewers V, Nielsen J (2016) Production of fatty acid-derived oleochemicals and biofuels by synthetic yeast cell factories. Nat Commun 7:11709
- Zhu Z, Zhou YJ, Kang MK, Krivoruchko A, Buijs NA, Nielsen J (2017) Enabling the synthesis of medium chain alkanes and 1-alkenes in yeast. Metab Eng 44:81–88

**Publisher's note** Springer Nature remains neutral with regard to jurisdictional claims in published maps and institutional affiliations.